

# Nonlinear Reduced Models for Control Design of Flexible-Free Flying Aircraft

N. D. Tantaroudas \*

*University of Liverpool, Liverpool, L69 3GH, United Kingdom*

A. Da.Ronch †

*University of Southampton, Southampton, S017 1BJ, United Kingdom*

K. J. Badcock ‡

*University of Liverpool, Liverpool, L69 3GH, United Kingdom*

Y. Wang § R. Palacios ¶

*Imperial College, London, SW7 2AZ, United Kingdom*

This paper describes a systematic approach to nonlinear model order reduction of free-flying aircraft and the subsequent flight control design. System nonlinearities arise due to large wing deformation and the coupling between flexible and rigid body dynamics. The non-linear flight dynamics equations are linearised and the approach uses information on the eigenspectrum of the resulting coupled system Jacobian matrix and projects it through a series expansion onto a small basis of eigenvectors representative of the full-order dynamics. The testcase is the very flexible wing representative of the Helios wing which was developed by NASA and the aeroelastic solver is validated against other frameworks for gust responses. Nonlinear reduced order models are generated and used for faster parametric worst case gust searches of the full order nonlinear flight dynamic response and are exploited for complex control methodologies such as  $H_\infty$ ,  $H_2$  and adaptive control designs.

## Nomenclature

$b$	= semi-chord
$x_\alpha$	= aerofoil static unbalance, $S_\alpha/m b$
$\mathbf{R}$	= residual vector
$c_h$	= non-dimensional distance from the mid-chord to the flap hinge
$U_\infty$	= freestream velocity
$U_L$	= linear flutter speed
$\rho_\infty$	= freestream density
$\mathbf{w}$	= vector of unknowns
$\mathbf{A}, \mathbf{B}, \mathbf{C}$	= first, second and third order Jacobian operators
$\mathbf{B}_c, \mathbf{B}_w$	= control, and disturbance recuded vector
$w_g$	= gust vertical normalized velocity

\*Ph.D. Student, School of Engineering; ntanta@liverpool.ac.uk (Corresponding Author).

†Lecturer, Faculty of Engineering and the Environment; Member AIAA.

‡Professor, School of Engineering. Senior Member AIAA.

§Graduate Research Assistant, Department of Aeronautics, AIAA Student Member

¶Reader, Department of Aeronautics. Member AIAA.

$W_0$	= intensity of gust vertical velocity
$L, M$	= lift and pitch moment
$w_1, \dots, w_8$	= augmented aerodynamic states for each deformable aerofoil section

*Greek*

$\alpha$	= angle of attack
$\delta$	= trailing-edge flap deflection
$\Psi$	= matrix of left coupled system eigenvectors
$\Phi$	= matrix of right coupled system eigenvectors

## I. Introduction

The accident of Nasa Helios flight mishap in 2003 triggered an increased interest for greater understanding of the fluid-structural coupling that occurs in light, very flexible and high aspect ratio wings.<sup>1</sup> The usual separation of flight dynamics and linear aeroelastic analysis is not appropriate for gust response predictions or flight control design when very low structural frequencies which are also often associated with large amplitude motions are present. Thus, several researchers have been working towards the development of nonlinear aeroelastic toolboxes that can simulate nonlinear structural dynamics coupled with rigid body motion and linear 2D or 3D aerodynamics. Patil et al.<sup>2</sup> studied the open loop dynamics of a flying wing structure similar to that of Helios which is used in this investigation and found that flap positions used to trim the flexible aircraft differ greatly from those used to trim the rigid aircraft. The stability analysis of the coupled linearised system was investigated and the instability in the phugoid mode was captured which is present during large dihedral angles and that was the main reason of Helios structural failure. Many other researchers have had similar findings and confirmed this result,<sup>3,4</sup> and more recently.<sup>5</sup> Other authors tried to experimentally validate their toolboxes by building an unmanned very flexible UAV called X-HALE<sup>6</sup> and more flight tests are to be done in the future<sup>7</sup> while a detailed description of the nonlinear flight dynamics of very flexible aircraft was first presented in.<sup>8</sup>

Large wing deformation brings nonlinear behaviour, but current model reduction methods assume linearity, or at most weak nonlinearity.<sup>9</sup> Previous work by the authors has focused on the generation of nonlinear reduced models that can capture this nonlinearity and be parametrised with respect to the flow conditions (freestream speed, density etc)<sup>10,11,12</sup>. The reduced models were used for control law design based on  $H_\infty$  for gust load alleviation and common pole-placement techniques for flutter suppression. Recently, a nonlinear control design methods was tested for a nonlinear experimental wind-tunnel rig for LCO suppression and was compared against conventional linear techniques.<sup>13</sup> Ideally though, a controller that can adapt during changes of the flow conditions such as airspeed or density is desired. Recent advances in adaptive control and especially in  $L_1$  adaptive control theory made possible the application of adaptive controllers for the control of uncertain non linear systems.<sup>14</sup> This design uses a state predictor similar to indirect model reference adaptive systems however the control input is obtained by filtering the estimated control signal with a low pass filter.  $L_1$  adaptive approach has been applied for the wing-rock control<sup>15</sup> and missile control.<sup>16</sup> In<sup>17</sup> an  $L_1$  adaptive controller for a prototypical pitch-plunge 2-D aeroelastic system in the presence of gust loads was developed. Other techniques of adaptive control such as model reference adaptive control have been applied at a flexible aircraft problem by using a rigid aircraft as a reference model and a neural network adaptation to control the structural flexible modes and compensate for the effects of unmodeled dynamics.<sup>18</sup> Recently Chowdhary et al.<sup>19</sup> presented flight tests results for adaptive controllers based on the MRAC architecture on the Georgia Tech GT Twinstar fixed wing engine aircraft with 25% of the wing missing. A recent promising adaptive control architecture was based on the derivative free MRAC<sup>20</sup> method. Recent work by the authors shown how the nonlinear reduced models can be used for model reference adaptive control design for gust load alleviation of a three degrees-of-freedom aerofoil model and for an unmaned aerial vehicle.<sup>21</sup> The controller was applied on the full order nonlinear system and the adaptation parameter selection was investigated together with the effect it had on the control input actuation.

The objective of this investigation is to validate the nonlinear aeroelastic toolbox developed, build on previous validations attempted by the authors for the rigid flight dynamics with the CFD and potential

aerodynamics<sup>22</sup> and finally combine all previous work done based on  $H_\infty$  and adaptive control to design flight control systems based on nonlinear reduced models capable of capturing the nonlinear flight dynamic effect of the full order system under large wing deformations.

The paper continues with an overview of the nonlinear coupled system of equations in § II. The model reduction is formulated in § III. The flexible aircraft model is presented in § V and reduced model are generated for the rigid flying wing cases. Finally, expected results for the conference manuscript are summarized in § VI.

## II. Nonlinear Coupled System of Equations

The general form of the fully coupled nonlinear model for the description of the flight dynamics of a very flexible aircraft can be represented in state-space form. Denote by  $\mathbf{w}$  the  $n$ -dimensional state-space vector which is conveniently partitioned into fluid, structural and rigid body degrees of freedom.

$$\mathbf{w} = (\mathbf{w}_f^T, \mathbf{w}_s^T, \mathbf{w}_r^T) \quad (1)$$

The state-space equations in the general vector form are

$$\frac{d\mathbf{w}}{dt} = \mathbf{R}(\mathbf{w}, \mathbf{u}_c, \mathbf{u}_d) \quad (2)$$

where  $\mathbf{R}$  is the nonlinear residual,  $\mathbf{u}_c$  is the input vector (e.g. control flap deflections or thrust) and  $\mathbf{u}_d$  is the exogenous vector for the description of some form of disturbance acting on the system (e.g. gust). The homogeneous system has an equilibrium point,  $\mathbf{w}_0$ , for given constant  $\mathbf{u}_{c0}$  and  $\mathbf{u}_{d0} = 0$  corresponding to a constant solution in the state-space and satisfying

$$\frac{d\mathbf{w}_0}{dt} = \mathbf{R}(\mathbf{w}_0, \mathbf{u}_{c0}, \mathbf{u}_{d0}) = 0 \quad (3)$$

The residual form in Eq. (3) forms the reference for the model reduction described below. The system is often parametrized in terms of an independent parameter (freestream-speed, air density, altitude, etc.) for stability analysis. The options for the residual evaluation are described in the next section.

### A. Linear Aerodynamic Model

A cheaper computational alternative to the computational fluid dynamics (CFD) valid for an irrotational and incompressible two-dimensional flow is the aerodynamic model given by the classical theory of Theodorsen.<sup>23</sup> This is a reasonable assumption when dealing with low-speed flow characteristics in 2-D. The total unsteady aerodynamic forces and moments can be separated into three components, circulatory, non-circulatory due to the wing motion and a contribution from the gust disturbance. The aerodynamic loads due to an arbitrary input time-history are obtained through convolution against a kernel function. For the influence of aerofoil motion on the loads, the Wagner function is used.<sup>24</sup> In a similar way, the influence of the gust is performed by introducing the Küssner function.<sup>25</sup> Since the assumption is of linear aerodynamics, the effects of both influences are added together to find the variation of the forces and moments for a given motion and gust. For a practical evaluation of the integral, a two lag exponential approximation is used for the Wagner and Küssner functions.

### B. Coupled Finite Element Equations of Motion

For the structural model, the geometrically-exact nonlinear beam equations are used.<sup>26</sup> Results are obtained using two-noded displacement-based elements. In a displacement-based formulation, nonlinearities arising from large deformations are cubic terms, as opposed to an intrinsic description where they appear up to second order. The nonlinear beam code was coupled with strip aerodynamics. The motion of each structural node is described by 6 degrees-of-freedom. The coupling between aerodynamic and structural models is performed considering that each structural node coincides with an aerodynamic section. No aeroelastic interface is required in this case, as the aerodynamic forces and moments are applied directly on each structural node. The system states follows first the structural degrees-of-freedom, then 6 rigid body degrees-of-freedom

followed by the 4 quaternions for the propagation of the beam with respect to the inertial frame and 8 augmented aerodynamic states for each deformable aerofoil section.

The dynamic equations of the coupled structural/flight model are written

$$\mathbf{M}(\mathbf{w}_s) \begin{bmatrix} \ddot{\mathbf{w}}_s \\ \ddot{\mathbf{w}}_r \end{bmatrix} + \mathbf{Q}_{gyr}(\dot{\mathbf{w}}_s, \mathbf{w}_s, \mathbf{w}_r) \begin{bmatrix} \dot{\mathbf{w}}_s \\ \dot{\mathbf{w}}_r \end{bmatrix} + \mathbf{Q}_{stiff}(\mathbf{w}_s) \begin{bmatrix} \mathbf{w}_s \\ \mathbf{w}_r \end{bmatrix} = \mathbf{R}_F(\ddot{\mathbf{w}}_s, \dot{\mathbf{w}}_s, \mathbf{w}_s, \ddot{\mathbf{w}}_r, \dot{\mathbf{w}}_r, \mathbf{w}_r, \mathbf{w}_f, \zeta_i, \mathbf{u}_c) \quad (4)$$

The subscripts  $S$  and  $R$  denote elastic and rigid-body properties respectively. The gyroscopic, elastic and external or aerodynamic forces is also discretised into elastic and rigid-body contributions respectively

$$\mathbf{Q}_{gyr} = \begin{pmatrix} \mathbf{Q}_{gyr}^s \\ \mathbf{Q}_{gyr}^r \end{pmatrix}, \quad \mathbf{Q}_{stiff} = \begin{pmatrix} \mathbf{Q}_{stiff}^s \\ 0 \end{pmatrix}, \quad \mathbf{Q}_{ext} = \begin{pmatrix} \mathbf{Q}_{ext}^s \\ \mathbf{Q}_{ext}^r \end{pmatrix} \quad (5)$$

The basic body reference frame and the frozen deformed geometry of a free-flying aircraft are given in Fig. 1

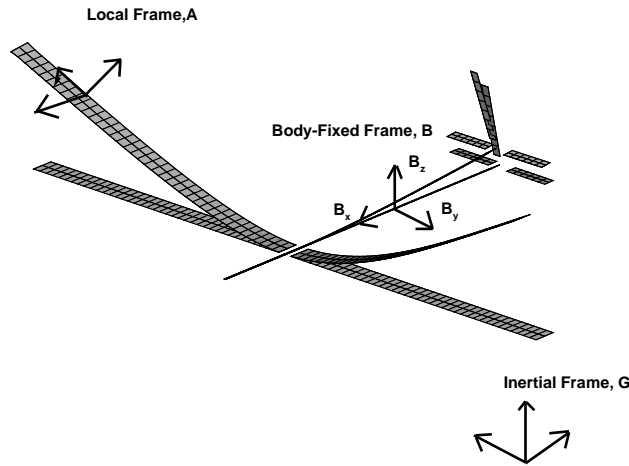


**Figure 1. Body reference frame and vehicle deformed coordinates**

The global Eq. (4) can be linearised from both sides and become coupled with the linearised quaternions and the augmented aerodynamic states.

$$\mathbf{M}_T \ddot{\mathbf{q}} + \mathbf{C}_T \dot{\mathbf{q}} + \mathbf{K}_T \mathbf{q} = \mathbf{D}_{FS} \mathbf{w}_f + \mathbf{B}_{CS} \mathbf{u}_c + \mathbf{D}_{FR} \mathbf{w}_f + \mathbf{B}_{cR} \mathbf{u}_c \quad (6)$$

$$\dot{\zeta}_i + \mathbf{C}_{QR} \dot{\mathbf{w}}_r + \mathbf{C}_{QQ} \zeta_i = 0 \quad (7)$$

$$\dot{\mathbf{w}}_f = \mathbf{A}_{fs} \mathbf{q} + \mathbf{A}_{ff} \mathbf{w}_f + \mathbf{A}_{fc} \mathbf{u}_c + \mathbf{A}_{fg} \mathbf{u}_d \quad (8)$$

A new state vector is defined such as  $\mathbf{x}_{new} = (\mathbf{q}, \dot{\mathbf{q}}, \zeta_i, \mathbf{w}_f)$  Then by taking the derivative of the new state vector and using the above equations which are coupled the system is recasted as a first order ODE as

follows.

$$\begin{pmatrix} \mathbf{q} \\ \dot{\mathbf{q}} \\ \dot{\zeta}_i \\ \dot{w}_f \end{pmatrix} = \begin{pmatrix} 0 & I & 0 & 0 \\ -M_T^{-1} \mathbf{K}_T & -M_T^{-1} \mathbf{C}_T & 0 & M_T^{-1} \mathbf{D}_{FS} + M_T^{-1} \mathbf{D}_{FR} \\ 0 & -\mathbf{C}_{QR} & -\mathbf{C}_{QQ} & 0 \\ \mathbf{A}_{fs} & 0 & 0 & \mathbf{A}_{fs} \end{pmatrix} \begin{pmatrix} \mathbf{q} \\ \dot{\mathbf{q}} \\ \zeta_i \\ \mathbf{w}_f \end{pmatrix} + \begin{pmatrix} 0 \\ M_T^{-1} \mathbf{B}_{CS} + M_T^{-1} \mathbf{B}_{CR} \\ 0 \\ \mathbf{A}_{fs} \end{pmatrix} \mathbf{u}_c + \begin{pmatrix} 0 \\ 0 \\ 0 \\ \mathbf{A}_{fg} \end{pmatrix} \mathbf{u}_g \quad (9)$$

The solution of the eigenvalue problem of Eq. (9) provides insight on the stability of the nonlinear system at the equilibrium point the linearisation was performed and can be used to construct the basis for the free-flying nonlinear model order reduction.

### III. Nonlinear Model Order Reduction

Denote  $\Delta \mathbf{w} = \mathbf{w} - \mathbf{w}_0$  the increment in the state-space vector with respect to an equilibrium solution. The large-order nonlinear residual is expanded in a Taylor series around the equilibrium point

$$\mathbf{R}(\mathbf{w}) \approx \mathbf{A} \Delta \mathbf{w} + \frac{\partial \mathbf{R}}{\partial \mathbf{u}_c} \Delta \mathbf{u}_c + \frac{\partial \mathbf{R}}{\partial \mathbf{u}_d} \Delta \mathbf{u}_d + \frac{1}{2} \mathbf{B}(\Delta \mathbf{w}, \Delta \mathbf{w}) + \frac{1}{6} \mathbf{C}(\Delta \mathbf{w}, \Delta \mathbf{w}, \Delta \mathbf{w}) + \mathcal{O}(|\Delta \mathbf{w}|^4) \quad (10)$$

retaining terms up to third order in the perturbation variable to describe the nonlinear full order dynamics. The Jacobian matrix of the system is denoted as  $\mathbf{A}$  and the vectors  $\mathbf{B}$  and  $\mathbf{C}$  indicate, respectively, the second and third order Jacobian operators. The control surface deflection and gust disturbance is indicated by  $\mathbf{u}_c$  and  $\mathbf{u}_d$ , respectively.

$$\mathbf{A} \mathbf{x} = \frac{\mathbf{R}_1 - \mathbf{R}_{-1}}{2\epsilon} \quad (11)$$

$$\mathbf{B}(\mathbf{x}, \mathbf{x}) = \frac{\mathbf{R}_1 - 2\mathbf{R}_0 + \mathbf{R}_{-1}}{\epsilon^2} \quad (12)$$

$$\mathbf{C}(\mathbf{x}, \mathbf{x}, \mathbf{x}) = \frac{-\mathbf{R}_3 + 8\mathbf{R}_2 - 13\mathbf{R}_1 + 13\mathbf{R}_{-1} - 8\mathbf{R}_{-2} + \mathbf{R}_{-3}}{8\epsilon^3} \quad (13)$$

where  $\mathbf{R}_l = \mathbf{R}(\mathbf{x}_0 + l\epsilon \Delta \mathbf{x})$ .

The full order system is projected onto a basis formed by a small number of eigenvectors of the Jacobian matrix evaluated at the equilibrium position. Right and left eigenvectors are scaled to satisfy the biorthonormality condition, see .<sup>10</sup> The projection of the full order model is done using a transformation of coordinates

$$\Delta \mathbf{w} = \Phi \mathbf{z} + \bar{\Phi} \bar{\mathbf{z}} \quad (14)$$

where  $\mathbf{z}$  is the state space vector governing the dynamics of the reduced order system and  $\Phi$  is the modal matrix of right coupled system eigenvectors. The result is a system of uncoupled ordinary differential equations in  $\mathbf{z}$ . The dependencies of the residual on control surface deflection and gust are evaluated by finite differences. A clear choice for the basis is to use eigenvectors corresponding to structural modeshapes modified by the flow at the specific equilibrium point, which are readily available when tracking frequencies and modeshapes for increasing air speed. If required, the basis can be enhanced by including additional eigenvectors until convergence.

The advantages of the approach are that: 1) it can retain non-linear effects from the original full order model; 2) once created, it is independent of the gust formulation and one reduced model can be used for parametric searches; 3) it allows control design on a small non-linear system and offers the possibility to investigate non-linear control techniques; and 4) the approach is systematic because control design is done in the same way independently of the formulation of the full order model. This technique only requires a coupled system in first order form.

## IV. Control of Flexible Aircraft

### A. H-Infinity Synthesis

This section describes the  $H_\infty$  control design process for the nonlinear reduced models. The dynamics of the reduced model are written as usual in the general form as

$$\dot{\mathbf{x}}(t) = \mathbf{A}\mathbf{x}(t) + \mathbf{B}_c\mathbf{u}_c(t) + \mathbf{B}_{c1}\dot{\mathbf{u}}_c(t) + \mathbf{B}_{c2}\ddot{\mathbf{u}}_c(t) + \mathbf{B}_g\mathbf{u}_d(t) + \mathbf{F}_{NR}(\mathbf{x}) \quad (15)$$

where  $\mathbf{F}_{NR}(\mathbf{x})$  contains the nonlinear terms of the reduced model. The matrix  $\mathbf{A}$  contains the eigenvalues of the coupled reduced system and  $\mathbf{B}_c, \mathbf{B}_{c1}, \mathbf{B}_{c2}$  are the control derivatives corresponding to rotation, angular velocity and angular acceleration of the control surfaces. The gust terms are given in  $\mathbf{B}_g$ . The system is rewritten introducing the flap rotation and angular velocity into the state vector, with the angular acceleration as a control input.

$$\begin{aligned} \begin{pmatrix} \dot{\mathbf{x}} \\ \dot{\mathbf{u}}_c \end{pmatrix} &= \begin{pmatrix} \mathbf{A} & \mathbf{B}_c & \mathbf{B}_{c1} \\ \mathbf{0} & \mathbf{0} & \mathbf{1} \\ \mathbf{0} & \mathbf{0} & \mathbf{0} \end{pmatrix} \begin{pmatrix} \mathbf{x} \\ \mathbf{u}_c \\ \dot{\mathbf{u}}_c \end{pmatrix} + \begin{pmatrix} \mathbf{B}_{c2} \\ \mathbf{0} \\ \mathbf{1} \end{pmatrix} \ddot{\mathbf{u}}_c \\ &+ \begin{pmatrix} \mathbf{B}_g \\ \mathbf{0} \\ \mathbf{0} \end{pmatrix} \mathbf{u}_d(t) + \begin{pmatrix} \mathbf{F}_{NR}(\mathbf{x}) \\ \mathbf{0} \\ \mathbf{0} \end{pmatrix} \end{aligned} \quad (16)$$

Rewrite the above equation as

$$\dot{\mathbf{x}}_e(t) = \mathbf{A}_e\mathbf{x}_e(t) + \mathbf{B}_e\ddot{\mathbf{u}}_c(t) + \mathbf{D}_e\mathbf{u}_d(t) + \mathbf{F}_e(\mathbf{x}) \quad (17)$$

where  $\ddot{\mathbf{u}}_c$  is the flap angular acceleration. The output equation is derived from Eq. (14). Thus, the complete set of equations by disregarding the nonlinear part for the control problem design become

$$\dot{\mathbf{x}}_e(t) = \mathbf{A}_e\mathbf{x}_e(t) + \mathbf{D}_e\mathbf{u}_d(t) + \mathbf{B}_e\ddot{\mathbf{u}}_c(t) \quad (18)$$

$$\mathbf{y}_{ctl}(t) = \mathbf{C}_1\mathbf{x}_e(t) + \mathbf{D}_{11}\mathbf{u}_d(t) + \mathbf{D}_{12}\ddot{\mathbf{u}}_c(t) \quad (19)$$

$$\mathbf{y}_{meas}(t) = \mathbf{C}_2\mathbf{x}_e(t) + \mathbf{D}_{21}\mathbf{u}_d(t) + \mathbf{D}_{22}\ddot{\mathbf{u}}_c(t) \quad (20)$$

where  $\mathbf{C}_1, \mathbf{C}_2$  are the representative eigenvectors of the reduced order model dynamics. The  $H_\infty$  control problem with additional input-shaping techniques for control tuning purposes for the classical  $H_\infty$  problem formulation is written<sup>27</sup>

$$\begin{pmatrix} \dot{\mathbf{x}}_e \\ \mathbf{y}_{ctl} \\ \mathbf{y}_{meas} \end{pmatrix} = \begin{pmatrix} \mathbf{A}_e & \mathbf{D}_e & \mathbf{B}_e \\ \mathbf{C}_1 & \mathbf{D}_{11} & \mathbf{D}_{12} \\ \mathbf{C}_2 & \mathbf{D}_{21} & \mathbf{D}_{22} \end{pmatrix} \begin{pmatrix} \mathbf{x}_e \\ \mathbf{u}_d \\ \ddot{\mathbf{u}}_c \end{pmatrix} \quad (21)$$

The output is distinguished by what the controller is aiming to control  $\mathbf{y}_{ctl}$  and what the controller has information about  $\mathbf{y}_{meas}$  which in that case is the aircraft angle of attack. The resulting controller has the linear form

$$\mathbf{u}(s) = \mathbf{K}(s)\mathbf{y}_{meas}(s) \quad (22)$$

where  $\mathbf{K}(s)$  is the  $H_\infty$  controller transfer function in the Laplace domain. It is one that aims to minimise the transfer of the disturbance signal from  $\mathbf{u}_d$  to  $\mathbf{y}_{ctl}$  by creating a controller that uses information from  $\mathbf{y}_{meas}$  to change the input  $\mathbf{u}_c$ . This can be written as

$$\frac{\sup \int_0^\infty \|\mathbf{y}_{meas}(t)\|^2 dt}{\sup \int_0^\infty \|\mathbf{u}_d(t)\|^2 dt} \leq \gamma \quad (23)$$

where  $\gamma$  represents the ratio of the maximum output energy to the maximum input energy. The problem is expanded to include a weight on inputs ( $\mathbf{K}_c$ ) which carries over to an additional element on controlled output and a weight on measurement noise ( $\mathbf{K}_d$ ) which carries over to an additional element on measured output. The  $H_\infty$  control is derived based on the linearized model and is applied directly to the nonlinear model by utilizing the reduced matrices from the nonlinear model order reduction framework.

## B. Model Reference Adaptive Control

This section describes how linear and nonlinear reduced models are used to design control laws based on model reference adaptive control. The stability proof of this methodology is well known.<sup>28</sup> This approach assumes an ideal reference model which will induce some constraints on the response of the actual aeroelastic system. The dynamics of the reduced model are given by Eq. (24)

$$\mathbf{x}(t)' = \mathbf{A}\mathbf{x}(t) + \mathbf{B}_c\mathbf{u}_c(t) + \mathbf{B}_g\mathbf{u}_d(t) + \mathbf{F}_{NR}(\mathbf{x}) \quad (24)$$

The assumed ideal model reference follows dynamics of the form

$$\mathbf{x}_m(t)' = \mathbf{A}_m\mathbf{x}_m(t) + \mathbf{B}_m\mathbf{u}_c(t) + \mathbf{B}_g\mathbf{u}_d(t) + \mathbf{F}_{NR}(\mathbf{x}_m) \quad (25)$$

The nonlinearity in the reference model has been selected to satisfy  $\mathbf{F}_{NR}(\mathbf{x}) = \mathbf{F}_{NR}(\mathbf{x}_m) = \mathbf{F}_{NR}$ . Matrix  $\mathbf{A}_m$  is a stable Hurwitz matrix that satisfies the desired properties of the reference system. This could mean eigenvalues with increased damping compared to the actual aeroelastic system. Matrix  $\mathbf{B}_m$  is user defined and describes the influence of the control inputs on the states of the reference model. The states of the reference model due to the increased damping in matrix  $\mathbf{A}_m$  will decay to zero faster under the same disturbances or flap actuation while their magnitude will be smaller as well. The goal is to find a dynamic control input  $\mathbf{u}_c(t)$  such that  $\lim_{t \rightarrow \infty} \|\mathbf{y}(t) - \mathbf{y}_m(t)\|$ . The exact control feedback for the model matching conditions is defined as

$$\mathbf{u}_c(t) = \mathbf{K}_x^*\mathbf{x}(t) + \mathbf{K}_r^*\mathbf{r}(t) \quad (26)$$

Eq. (24) and satisfying the model matching conditions yields

$$\begin{aligned} \mathbf{A} + \mathbf{B}_c\mathbf{K}_x^* &= \mathbf{A}_m \\ \mathbf{B}_c\mathbf{K}_r^* &= \mathbf{B}_m \end{aligned} \quad (27)$$

Since  $\mathbf{A}$  and  $\mathbf{B}_c$  are considered to be unknown to the controller the values denoted in Eq. (26) (e.g  $\mathbf{K}_x^*$ ,  $\mathbf{K}_r^*$ ) are also unknown at initial time and the actual control signal applied at the current timestep is defined as

$$\mathbf{u}_c(t) = \mathbf{K}_x(t)\mathbf{x}(t) + \mathbf{K}_r(t)\mathbf{r}(t) \quad (28)$$

The gains  $\mathbf{K}_x(t)$  and  $\mathbf{K}_r(t)$  in Eq.(28) are dynamic gains that need to be solved and at the end will be required to converge to the values that provide a solution to Eq. (27). The closed loop dynamics of the nonlinear reduced model at this point can be expressed as

$$\mathbf{x}(t)' = (\mathbf{A} + \mathbf{B}_c\mathbf{K}_x(t))\mathbf{x}(t) + \mathbf{B}_c\mathbf{K}_r(t)\mathbf{r}(t) + \mathbf{B}_g\mathbf{u}_d(t) + \mathbf{F}_{NR} \quad (29)$$

Let  $\theta^* = [\mathbf{K}_x^* \ \mathbf{K}_r^*]^T$  and  $\theta = [\mathbf{K}_x(t) \ \mathbf{K}_r(t)]^T$ . The estimation error between the instantaneous and the ideal gains is defined as

$$\bar{\theta} = \theta^* - \theta = (\bar{\theta}_x \ \bar{\theta}_r)^T \quad (30)$$

with  $\bar{\theta}_x = \mathbf{K}_x^* - \mathbf{K}_x(t)$ ,  $\bar{\theta}_r = \mathbf{K}_r^* - \mathbf{K}_r(t)$ . Now define  $\phi = \left(\mathbf{x}(t)^T \ \mathbf{r}(t)\right)^T$ . In that case the closed loop system dynamics in Eq. (29) are expressed as

$$\begin{aligned} \mathbf{x}(t)' &= (\mathbf{A} + \mathbf{B}_c\mathbf{K}_x^*)\mathbf{x}(t) + \mathbf{B}_c\mathbf{K}_r^*\mathbf{r}(t) - \mathbf{B}_c\bar{\theta}_x\mathbf{x}(t) - \mathbf{B}_c\bar{\theta}_r\mathbf{r}(t) + \mathbf{B}_g\mathbf{u}_d(t) + \mathbf{F}_{NR} \\ &= \mathbf{A}_m\mathbf{x}(t) + \mathbf{B}_m\mathbf{r}(t) - \mathbf{B}_c\phi^T\bar{\theta} + \mathbf{B}_g\mathbf{u}_d(t) + \mathbf{F}_{NR} \end{aligned} \quad (31)$$

For the purpose of the stability proof of the closed loop system one needs to define the error dynamics between the two systems.

$$\mathbf{e}(t) = \mathbf{x}(t) - \mathbf{x}_m(t) \quad (32)$$

The derivative of which, expresses the rate of change between the two systems and can be written as

$$\begin{aligned} \mathbf{e}(t)' &= \mathbf{x}(t)' - \mathbf{x}_m(t)' \\ &= \mathbf{A}_m\mathbf{x}(t) + \mathbf{B}_m\mathbf{r}(t) - \mathbf{B}_c\phi^T\bar{\theta} + \mathbf{F}_{NR} - \mathbf{A}_m\mathbf{x}_m(t) - \mathbf{B}_m\mathbf{r}(t) - \mathbf{F}_{NR} + \mathbf{B}_g\mathbf{u}_d(t) - \mathbf{B}_g\mathbf{u}_d(t) \\ &= \mathbf{A}_m(\mathbf{x}(t) - \mathbf{x}_m(t)) - \mathbf{B}_c\phi^T\bar{\theta} \\ &= \mathbf{A}_m\mathbf{e}(t) - \mathbf{B}_c\phi^T\bar{\theta} \end{aligned} \quad (33)$$

The Lyapunov equation is solved for the reference model and its solution will be part of the steady part of the Lyapunov candidate function that will lead to the stability proof of the nonlinear reduced model.

$$PA_m + A_m^T P = -Q, \quad Q = Q^T \geq 0 \quad (34)$$

where in Eq.(34)  $Q$  is a semi-definite positive user defined matrix. A scalar quadratic Lyapunov function  $V$  in  $e$  and  $\bar{\theta}$  may be defined, such that the system becomes asymptotically stable by satisfying  $V > 0$  and its time derivative is semi definite negative  $V' \leq 0$ <sup>28</sup>. This function will provide insight on the selection of the parameter update law of the time varying gains in Eq. (28). The Lyapunov function

$$V(e(t), \theta) = e(t)^T P e(t) + \bar{\theta}^T \Gamma^{-1} \bar{\theta} > 0 \quad (35)$$

is considered, where  $P = P^T > 0$  is the solution of the algebraic Lyapunov Eq. (34) for a particular selection of  $Q$  while  $\Gamma = \Gamma^T \geq 0$  is a user defined semi definite positive matrix. By calculating the derivate of the above Lyapunov candidate one can show that by selecting the following adaptation parameter, global asymptotic stability is guaranteed.

$$\bar{\theta}' = -\Gamma \phi e(t)^T P B_c \quad (36)$$

which leads to

$$V'(e(t), \theta) = -e(t)^T Q e(t) \leq 0 \quad (37)$$

which is valid due to the semi definite positiveness of matrix  $Q$ . The dynamic time varying gains in Eq. (28) are updated by the adaptive law so that the time derivative of the Lyapunov function decreases along the error dynamic trajectories as in Eq. (37). By using Barbalat's lemma this translates in boundness of the error dynamics with respect to the time evolution and as a result satisfaction of the model matching conditions. In general, this control approach is limited to minimum phase systems. Thus, when applied in unstable nonminimum phase systems unstable zero-pole cancelation may occur and the error between the two assumed models slowly diverges to infinity. However, a simple feedback based on the Bass-Gura formula<sup>29</sup> can be applied on the ROM to place any unstable zeros on the left half plane.

## V. Very Flexible Aircraft

This investigation is dealing with a very flexible aircraft which resembles the prototype HELIOS unmanned aerial vehicle developed by NASA. The 72-m span high-aspect ratio flying wing design was original created by Patil et al.<sup>2</sup> The wing is straight and forms a dihedral of 10 degrees towards the wing tip. Furthermore, payload is placed in the central pod and can be varied between 0 and 227 kg. To provide thrust forces, five propellers are mounted forward of the midscetion while three vertical fins are below it. Control surfaces with 20%chord length were assumed to run across the whole wing span. The structural

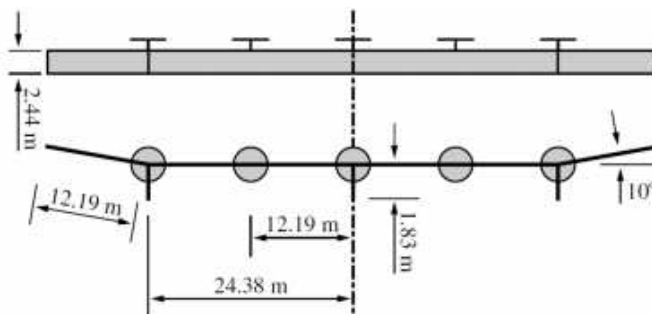


Figure 2. Flying Wing Geometry as in<sup>30</sup>

properties of the aircraft are summarised in Table 1

**Table 1. Helios-like wing structural properties**

Elastic/Reference axis	25% chord
Aerodynamic centre	25% chord
Centre of gravity	25% chord
$GJ$	$1.65 \times 10^5 \text{ Nm}^2$
$EI_2$	$1.03 \times 10^6 \text{ Nm}^2$
$EI_3$	$1.24 \times 10^7 \text{ Nm}^2$
$m$	$8.93 \text{ Kg/m}$
$I_{11}$	$4.15 \text{ kg m}$
$I_{22}$	$0.69 \text{ kg m}$
$I_{33}$	$3.46 \text{ kg m}$

## A. Nonlinear Model Reduction

The structural model of the wing is assembled by 60 beam elements and is coupled with 2D aerodynamics. The total dimension of the system thus becomes 1200 states together with the augmented aerodynamic states for each aerofoil section. A 1-cos gust was assumed at the flow conditions given in Table 2. The rational approximation documented in <sup>31</sup> can be used for the generation of continuous models of atmospheric Von Kármán turbulence. Two reduced models were generated at this flight condition. One model represents the

**Table 2. Flow conditions and gust properties**

Altitude	20.000 m
Freestream speed $U_\infty$	25.0 m/s
Density $\rho_\infty$	$0.0789 \text{ kg/m}^3$
Angle of attack $AoA$	0.0 degrees

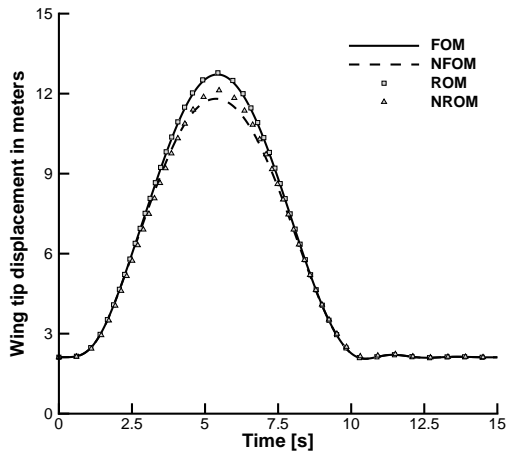
linearized aeroelastic system, and the other one includes the nonlinear terms up to second order. Both models were built using 14 modes for the projection. Since for a slender wing the coupling between flexural and torsional modes is low, the two lowest bending and the first torsional modes were included. Aerodynamics-dominated modes (related to gust disturbance) were then included. As a result, an overall significant reduction was achieved from 1200 states to 14 at the end. Figure 3 illustrates the time response of the wing tip vertical displacement for two sets of results for a shorter gust length with the same reduced models. The first set of data represents the system response when nonlinear flexibility effects are neglected. The linear reduced model is identical to the linearized full order model. The second set of results includes the nonlinear flexibility effects in both reduced and full models. Whereas deformations are very large (12.5 – 20m for a 36.0m wing span), the nonlinear reduced model is virtually identical to the reference solution.

In Fig. 4 the ability of the reduced models to predict aeroelastic responses under stochastic turbulence by Von Kármán is demonstrated showing that one ROM can be used systematically for parametric search being independent of the gust.

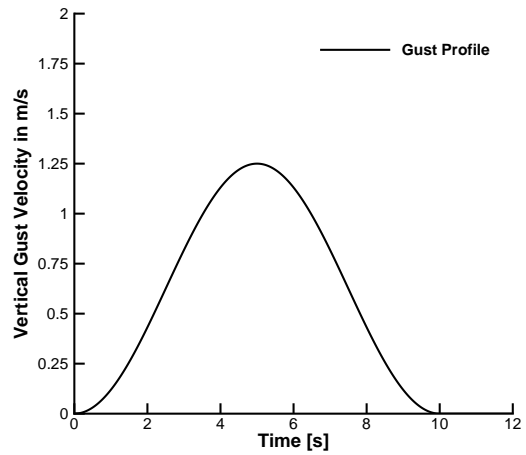
It is expected that the nonlinear dynamic effect will become apparent when there is coupling of rigid body motion with the structural dynamics for the free-flying aircraft case.

## B. Control Application

The reduced order models that have been generated are used for  $H_\infty$  and model reference adaptive control design. The resulting controller even though is based on the reduced model is directly applied on the nonlinear full order dynamics. For the derivation of the  $H_\infty$  controller, input shaping techniques were applied to get the best closed-loop performance as firstly discussed in <sup>11</sup> Furthermore, the performance of the model reference adaptive controller is strongly affected by the selection of the adaptation parameters  $Q$  and  $\Gamma$  as shown in section IV and investigated in <sup>21</sup>

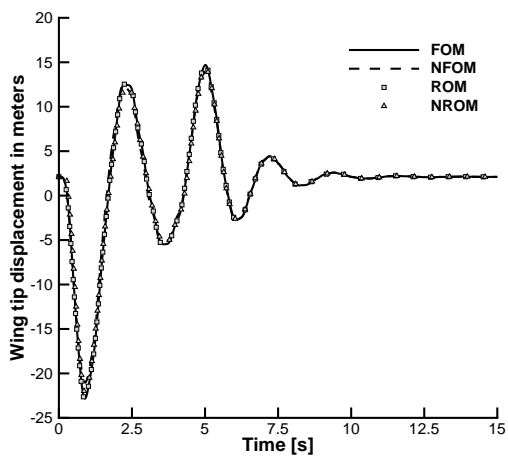


(a) Wing Tip displacement in meters

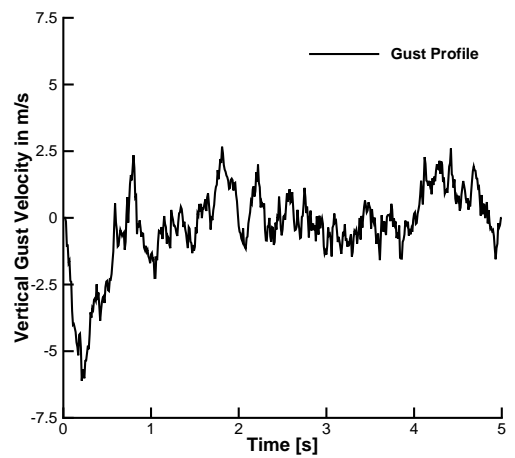


(b) "1-cosine" gust profile in m/s

Figure 3. Wing Tip Deformation in meters for "1-cosine" gust of intensity 5% of the freestream speed for full and reduced models for the flow conditions give in Table. 2



(a) Wing Tip displacement in meters



(b) "Stochastic Continuous Gust in m/s

Figure 4. Wing Tip Deformation in meters for stochastic turbulence for full and reduced models for the flowconditions given in Table 2

The closed-loop response of the wing tip for the two controllers for the case of the discrete "1-cosine" gust and the resulting flap angle are given in In Fig. 5. It is shown that the MRAC control design alleviates the gust loads as much as the  $H_\infty$  design. However, for a different selection of an adaptation parameter the model reference controller might produce worse results but in general is desired to be kept small in order to prevent an unrealistic flap angle actuation as discussed in <sup>21</sup>

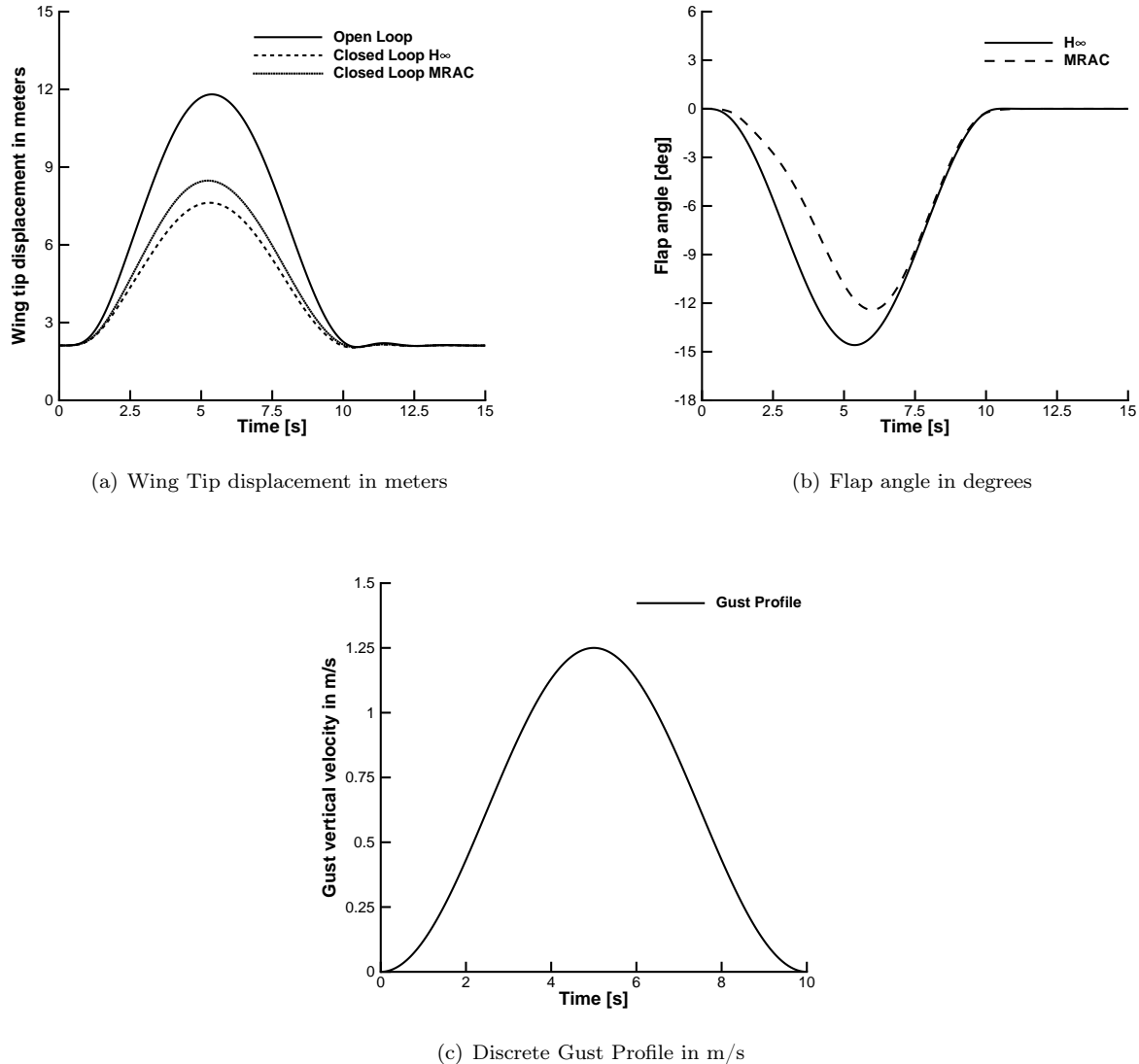
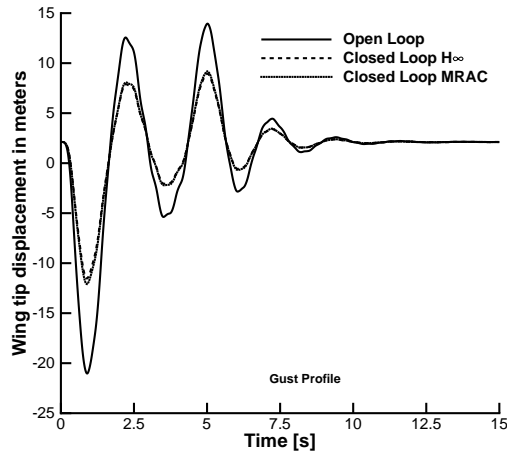


**Figure 5. Wing Tip deformation in meters for a "1-cosine" gust for full open-loop against the closed-loop designs**

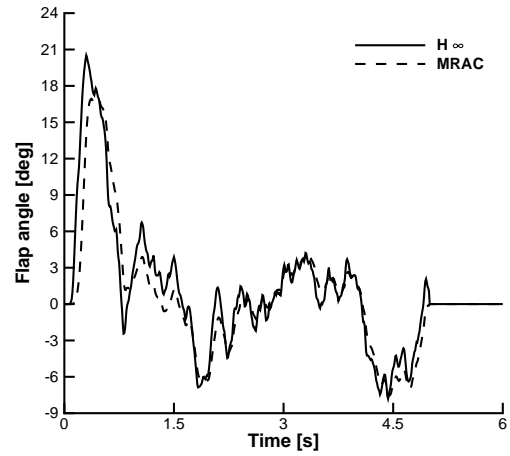
Both control implementations can also be applied in the presence of stochastic atmospheric turbulence. In Fig. 6 the wing tip displacements together with the closed-loop flap rotations are given for a Von Kármán stochastic gust.

### C. Flexible Free-Flying Aircraft

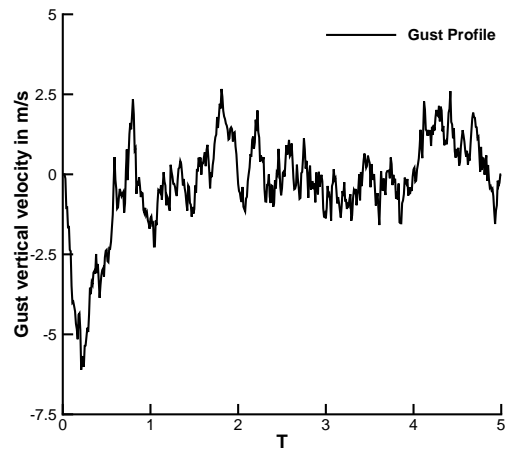
Rigid body motion introduces significant contributions in the aerodynamics of flexible free flying aircraft and needs to be taken into account. Following the Eq. (9), the system becomes coupled with 2D aerodynamics and can be integrated as 2nd order or 1st order nonlinear equation while the linearised eigenvalue solution of the above equation can provide insight of the stability of the nonlinear flight dynamics at the trimming position.



(a) Wing Tip Deformation in meters



(b) Flap angle in degrees



(c) Stochastic Gust Profile in m/s

Figure 6. Wing tip deformation in meters for stochastic turbulence for full open-loop against closed-loop designs

In Fig ?? the difference for a rigid aircraft compared to the free flying aircraft for a strong stochastic gust is shown. Gravitational forces in that case have been taken into account as they play as strong part in the stability of the flight dynamics.

## VI. Expected Results

### References

- <sup>1</sup>Brown, N. T. E., Perez-Davids, J., Ishmael, M., Tiffany, S., and Gaier, M., "Investigation of the Helios Prototype Aircraft Mishap Volume I:Mishap Report," *NASA*, 2004.
- <sup>2</sup>Patil, M. J. and Hodges, D. H., "Flight dynamics of highly flexible flying wings," *Journal of Aircraft*, Vol. 43, No. 6, 2006, pp. 1790–1799.
- <sup>3</sup>Su, W. and Cesnik, C. E., "Dynamic response of highly flexible wings," *Proceedings of the 47th AIAA/ASME/ASCE/AHS/ASC Structural Dynamics and Materials Conference*, 2006.
- <sup>4</sup>Raghavan, B. and Patil, M., "Flight Dynamics of Highly Flexible Flying Wings," *Journal of Aircraft*, Vol. Vol 43, No. No.6, 2006.
- <sup>5</sup>Wang, Y., Wynn, A., and Palacios, R., "Nonlinear Model Reduction for Aeroelastic Control of Flexible Aircraft Described by Large Finite-Element Models," *AIAA Paper Scitech 2014*, 13-17 January 2014.
- <sup>6</sup>Cesnik, C. and Su, W., "Nonlinear Aeroelastic Simulation of X-HALE:a very Flexible UAV," *AIAA 2011-1226*.
- <sup>7</sup>Cesnik C.E.S. Senatore P.J. Su W. Atkins E.M., Shearer, C. and Pitcher, N., "X-HALE:A Very Flexible UAV for Nonlinear Aeroelastic Tests," *AIAA 2010*.
- <sup>8</sup>Shearer, C. and Cesnik, C., "Nonlinear Flight Dynamics of Very Flexible Aircraft," *Journal of Aircraft*, Vol. Vol.44, No. No.5, 2007.
- <sup>9</sup>Silva, W., "Identification of Nonlinear Aeroelastic Systems based on the Volterra Theory: Progress and Opportunities," *Nonlinear Dynamics*, Vol. 39, No. 1–2, 2005, pp. 25–62, doi: 10.1007/s11071-005-1907-z.
- <sup>10</sup>Da Ronch, A., Badcock, K. J., Wang, Y., Wynn, A., and Palacios, R. N., "Nonlinear Model Reduction for Flexible Aircraft Control Design," *AIAA Atmospheric Flight Mechanics Conference*, AIAA Paper 2012–4404, 2012.
- <sup>11</sup>Da Ronch, A., Tantaroudas, N. D., and Badcock, K. J., "Reduction of Nonlinear Models for Control Applications," *Proceedings of the AIAA 54th Structures,Structural Dynamics and Materials Conference*, 08-11 April 2013.
- <sup>12</sup>Papathéou, E., Tantaroudas, N. D., Da Ronch, A., Cooper, J. E., and Mottershead, J. E., "Active Control for Flutter Suppression: An Experimental Investigation," 24-27 June, Bristol, UK 2013.
- <sup>13</sup>Da Ronch, A., Tantaroudas, N. D., Jiffri, S., and Mottershead, J., "A Nonlinear Controller for Flutter Suppression: from Simulation to Wing Tunnel Testing," *AIAA Paper Scitech 2014*, 13-17 January 2014.
- <sup>14</sup>Cao, C. and Hovakimyan, N., "Adaptive control for nonlinear systems in the presence of unmodelled dynamics:part II," *Proceedings of the American Control Conference, Seattle, WA*, pp. 4099–4104.
- <sup>15</sup>Cao, C. and Hovakimyan, N., " $L_1$  adaptive controller to wing rock," *In:Proceeding of AIAAA Guidance,Navigation and Control Conference AIAA*, 2006-6426 Keystone,CO.
- <sup>16</sup>Cao, C. and Hovakimyan, N., " $L_1$  adaptive output-feedback controller for non-strictly-positive-real reference systems:missile longitudinal autopilot design," *Journal of Guidance,Control,and Dynamics*, Vol. 32, pp. 717–726.
- <sup>17</sup>Keum, W. L. and Sahjendra, N. S., " $L_1$  adaptive control of a nonlinear aeroelastic system despite gust load," *Journal of Vibration and Control*, Vol. 0(0)1-15, 2012.
- <sup>18</sup>Ponnusamy, S. and Guibe, J., "Adaptive output feedback control of aircraft flexible modes," *2nd International Conference on Communications Computing and Control Applications,CCCA 2012*, Marseille,France 6 December.
- <sup>19</sup>Chowdhary, G., Johnson, E., Kimbrell, M., Chandramohan, R., and Calise, A., "Flight Test Results of Adaptive Controllers in Presence of Severe Structural Damage," *AIAA Guidance,Navigation and Control Conference*, 2010.
- <sup>20</sup>Yucelen, T. and Calise, A., "Derivative-Free Model Reference Adaptive Control of a Generic Transport Model," *AIAA Guidance Navigation and Control Conference*, 2 August 2010 through 5 August 2010.
- <sup>21</sup>Tantaroudas, N., Da Ronch, A., Gai, G., Badcock, K., Wang, Y., Hesse, H., and Palacios, R., "An Adaptive Aeroelastic Control Approach by using Non Linear Reduced Order Models," *AIAA Paper Aviation 2014*, 16-21 June 2014.
- <sup>22</sup>Da Ronch, A., McCracken, A., Tantaroudas, N., Badcock, K., Hesse, H., and Palacios, R., "Assessing the Impact of Aerodynamic Modelling on Manoeuvring Aircraft," *AIAA Paper Scitech 2014*, 13-17 January 2014.
- <sup>23</sup>Theodorsen, T., "General Theory of Aerodynamic Instability and the Mechanism of Flutter," *NACA Report Nr. 496*, 1935.
- <sup>24</sup>Jones, R. T., "The Unsteady Lift of a Wing of Finite Aspect Ratio," *NACA Report Nr. 681*, 1940.
- <sup>25</sup>Leishman, J. G., "Unsteady Lift of a Flapped Airfoil by Indicial Concepts," *Journal of Aircraft*, Vol. 31, No. 2, 1994, pp. 288–297.
- <sup>26</sup>Hesse, H. and Palacios, R., "Consistent Structural Linearisation in Flexible–body Dynamics with Large Rigid–body Motion." *Computers& Structures*, Vol. 110–111, No. 0, pp. 1–14.
- <sup>27</sup>Zhou, K. and Doyle, J. C., *Essentials of Robust Control*, New York:Prentice Hall, 1998.
- <sup>28</sup>Ioannou, P. A. and Sun, J., "Robust Adaptive Control," *Prentice- Hall*, 1996.
- <sup>29</sup>Ogata, K., "Modern Control Engineering," 2010.
- <sup>30</sup>Dillsaver, M. J., Cesnik, C. E. S., and Kolmanovsky, I., "Gust Response Sensitivity Characteristics of Very Flexible Aircraft," *AIAA Atmospheric Flight Mechanics Conference*, Minneapolis, Minnesota,AIAA, 2012, 13-16 August 2012.
- <sup>31</sup>Campbell, C., "Monte Carlo Turbulence Simulation Using Rational Approximations to von Karman Spectra," *AIAA Journal*, Vol. 24, No. No.1, 1986.